H-2-01
Extended Abstracts of the 2019 International Conference on Solid State Devices and Materials, Nagoya, 2019, pp359-360

Endurance Improvement in Ferroelectric Y-doped HfO_2 Thin Films on $NiSi_2$ with Low-Thermal Budget Processing

Joel Molina-Reyes[1,2*], Takuya Hoshii[1], Shun-Ichiro Ohmi[1], Hiroshi Funakubo[1], Atsushi Hori[1], Ichiro Fujiwara[1], Hitoshi Wakabayashi[1], Kazuo Tsutsui[1] and Kuniyuki Kakushima[1]

[1] Tokyo Institute of Technology
Yokohama 226-8502, Japan.
Phone: +81- 045-924-5471. E-mail: molina.j.aa@m.titech.ac.jp
[2] National Institute of Astrophysics, Optics and Electronics
Tonantzintla, Puebla, 72840, Mexico.
Phone: +52-2222663100. E-mail: jmolina@inaoep.mx

Abstract

We exploit the uniform silicidation of a Ni ultra-thin film deposited on silicon that upon annealing, transforms into $NiSi_2$ that is used as a bottom electrode with the right structure for crystallization of Y-doped HfO_2 (HYO) during post deposition annealing (PDA). By using $NiSi_2$ and PDA, ferroelectric behavior of HYO thin films is obtained while endurance shows that a 500°C-PDA TiN/HYO/$NiSi_2$ capacitor is able to withstand up to 10e8 stress cycles without reducing its remanent polarization (Pr).

1. Introduction

It has been demonstrated that the orthorhombic transformation of Si, Zr, or Y doped HfO_2 (induced by annealing) is responsible for its ferroelectricity (FE) but the use of capping top electrodes is usually required [1-4]. With a top metallic electrode, the metal-insulator-metal (MIM) capacitors generate high stress conditions during post-metallization annealing (PMA), which then crystallize the metal doped HfO_2 film into a mixed phase including the orthorhombic one. However, the use of PMA for FE development in HfO_2 thin films usually requires high thermal budgets able to produce high stressing between the top and bottom electrodes and thus, the desired orthorhombic transformation [1-2]. Here, we show that by using $NiSi_2$ as a bottom electrode (with a fluorite orthorhombic structure) [5] and PDA, not only FE properties of HYO thin films are obtained but also the endurance is enhanced. This way, instead of the expected "epitaxial-like" growth of the orthorhombic phase of HYO on $NiSi_2$ during PDA, a reduction in the oxide defects' density could improve the electrical and endurance properties for MIM capacitors annealed at 500 °C.

2. Device Fabrication and Characterization

Fig. 1 (a) shows the complete processing flow for fabrication of MIM capacitors where 7mol%Y:HfO_2 (HYO7) is directly deposited on top of $NiSi_2$. The Ni silicidation as well as the PDA treatments for the HYO7/$NiSi_2$ structures were done by rapid thermal annealing in argon using the ramping profile shown in (b). The bottom/top metallic films and the HYO7 are all deposited by sputtering at room temperature. Insets show a schematic and TEM image (HYO7= 22nm) of the fabricated MIM devices respectively. From TEM, a thin interfacial layer (IL, presumably SiO_2) is noticed at the interface of the HYO7/$NiSi_2$ structure, which could prevent a full crystallization of HYO7 starting from the $NiSi_2$ surface.

3. Results and Discussion

Fig. 2 shows X-ray diffraction peaks for HYO7/$NiSi_2$/Si structures after PDA. The inset zooms into 2θ= 29-31, where the combined orthorhombic, tetragonal and cubic (o/t/c) phases are found [4]. Although the 700 °C sample shows the highest peak (suggesting greater orthorhombic component), its Pr is the lowest from all samples as will be shown later. **Fig. 3** shows the leakage current density and remanent polarization for (a-c) TiN/HYO7/$NiSi_2$ and (b-d) TiN/HYO7/TiN structures after PDA at 400 °C respectively. High uniformity and lower leakage current is obtained when $NiSi_2$ is used as bottom electrode (BE). On the other hand, higher Pr is obtained with TiN used as BE. This is due to the lack of an IL at the HYO7/TiN interface (data not shown). If present, this IL could reduce orthorhombic transformation in HYO7 thus decreasing Pr. **Fig. 4** shows the polarization switching currents and capacitor charge currents (Ip, Ic) versus pulse time during PUND (Positive-Up-Negative-Down) measurements. PUND is able to extract the real switching polarization (Psw) in leaky devices. **Fig. 5** shows the influence of (a) PDA temperature and (b) applied wave frequency on Pr measurements. Here, the 600 °C sample shows higher Pr. It is important to notice the strong dependence of the applied wave frequency on Pr, which could increase to even larger Pr values by using lower frequencies during hysteresis measurements (suggesting high density of mobile oxygen vacancies). Finally, **Fig. 6** shows the endurance data for $NiSi_2$ and TiN based samples with applied electric fields of (a) 3 MV/cm and (b) 3.8 MV/cm. The TiN/HYO7/$NiSi_2$ sample annealed at 500 °C is able to withstand up to 10e8 stressing cycles at low and high applied E.

4. Conclusions

The use of $NiSi_2$ as a bottom electrode in FE-HYO7 and 500 °C PDA improved the endurance performance up to 10e8 stressing cycles. A HYO7/IL/$NiSi_2$ structure is useful for increasing the uniformity in electrical behavior (possibly reducing the density of defects) that could positively impact on the performance and reliability of ferroelectric tunnel junctions.

Acknowledgements

This research is supported by the Center of Innovation Program from Japan Science and Technology Agency, JST.

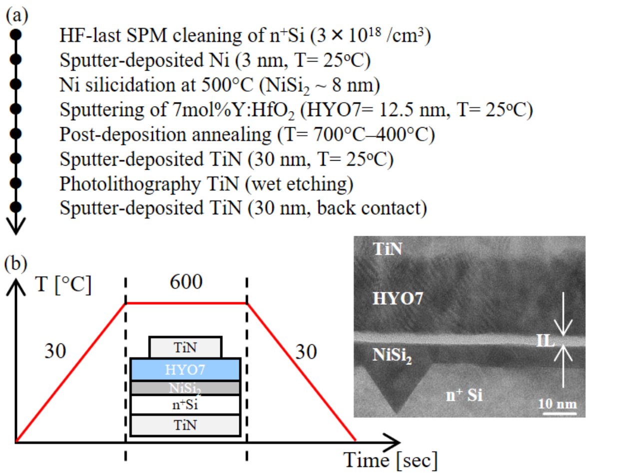

Fig. 1 a) Process flow for fabrication of HYO-MIM caps. b) PDA ramping profile for Ni silicidation and ferroelectric transformation of $Y:HfO_2/NiSi_2/Si$ structures. Left inset shows a schematic of the MIM capacitor and right inset a TEM image for the same MIM structure using a thicker HYO7 (22 nm).

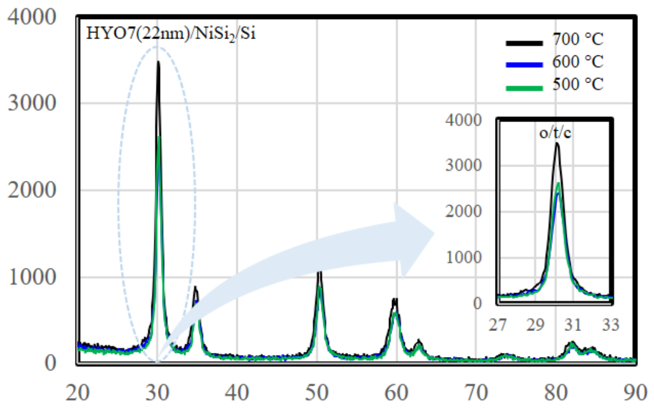

Fig. 2 In-plane XRD peaks for $7mol\%Y:HfO_2/NiSi_2/Si$ structures after PDA (HYO7= 22 nm). The inset shows a zoom-into the main crystalline peaks at 2θ=27-33° for HYO7 (consisting of o/t/c phases).

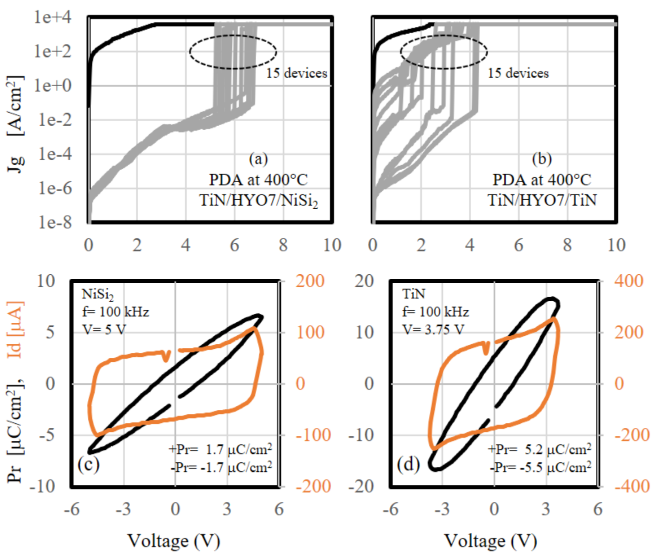

Fig. 3 Leakage current density, remanent polarization and displacement current (Jg, Pr, Id) for HYO7 (12.5 nm) using (a-c) $NiSi_2$ and (b) TiN as BE.

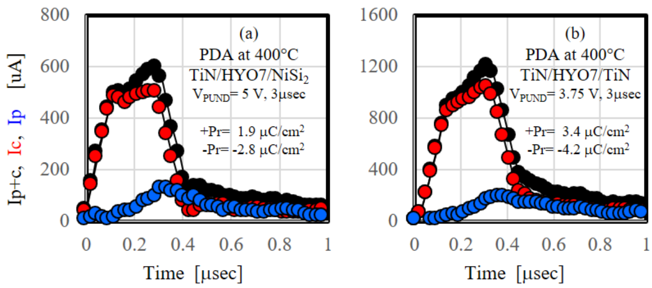

Fig. 4 Polarization switching current and capacitor charge current (Ip, Ic) versus pulse time during PUND measurements for (a) $NiSi_2$ and (b) TiN devices. PUND corrects an overestimation of ±Pr in leaky TiN devices.

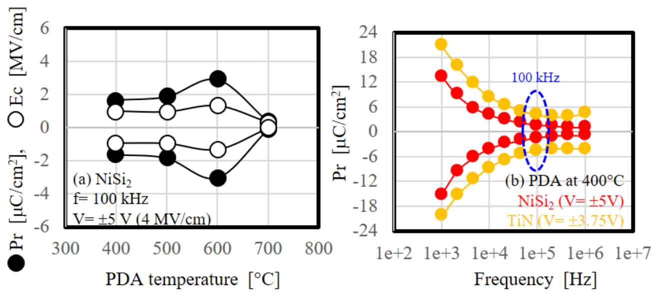

Fig. 5 (a) Influence of PDA temperature on remanent polarization and coercive field (Pr, Ec) for $TiN/HYO7/NiSi_2$ devices. (b) Influence of applied wave frequency on Pr measurement for $NiSi_2$ and TiN devices.

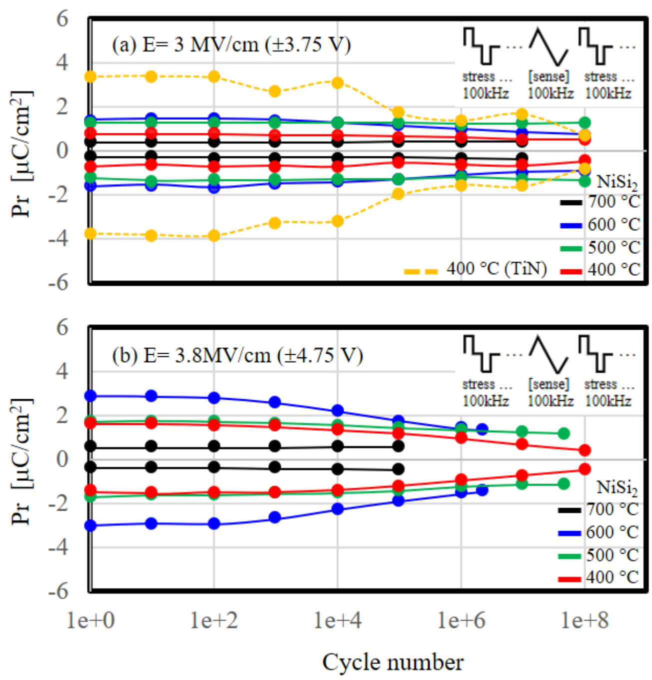

Fig. 6 Endurance measurements for HYO7-based MIM devices at (a) 3 MV/cm and (b) 3.8 MV/cm applied electric field E. Although a TiN/HYO7/TiN device shows initially higher Pr, $TiN/HYO7/NiSi_2$ devices are able to withstand up to 10e8 stressing cycles at low and high E without significantly reducing Pr (less fatigue).

References

[1] T. S. Boscke et al, IEDM, (2011) 547. [2] T. Onaya et al., ECS Transactions. **86** (2018) 6. [3] T. Shimizu et al., Sci. Rep., **6** (2016) 32931. [4] X. Tian et al., Appl. Phys. Lett. **112**, 102902 (2018). [5] N Ikarashi et al., J. Phys.: Conf. Ser. **326** (2011) 012051.